Journal of Electroanalytical Chemistry 782 (2016) 125–132

Contents lists available at ScienceDirect

Journal of Electroanalytical Chemistry

journal homepage: www.elsevier.com/locate/jelechem

The charge transport process at gold electrodes modified by thick nickel hydroxide films. A study employing rotating disc electrode voltammetry in the presence of the $Fe(CN)_6^{3-/4-}$ redox couple

R. Tucceri [1]

Instituto de Investigaciones Fisicoquímicas Teóricas y Aplicadas (INIFTA), Conicet, Facultad de Ciencias Exactas, Universidad Nacional de La Plata, Sucursal 4, Casilla de Correo 16, 1900 La Plata, Argentina

ARTICLE INFO

Article history:
Received 2 August 2016
Received in revised form 20 September 2016
Accepted 9 October 2016
Available online 11 October 2016

Keywords:
Nickel hydroxide films
Charge transport processes
$Fe(CN)_6^{3-/4-}$ species diffusion coefficient

ABSTRACT

Rotating disc electrode voltammetry (RDEV) was employed to study the transport properties of nickel hydroxide films electrochemically deposited on gold in the presence of the $Fe(CN)_6^{3-/4-}$ redox couple. Gold electrodes coated with nickel hydroxide surface coverages within the range 0.7 nmol $cm^{-2} < \Gamma_{Ni(OH)2} < 55$ nmol cm^{-2} were obtained. Steady-state current vs. potential (*I-E*) dependences at different electrode rotation rates within the range 50 rpm–5000 rpm were recorded for each $\Gamma_{Ni(OH)2}$ value. While the anodic limiting current at the different nickel hydroxide surface coverages followed the Levich equation, the cathodic limiting current only responded to the Levich relationship within the $\Gamma_{Ni(OH)2}$ range comprised between 0.7 nmol cm^{-2} and 16 nmol cm^{-2}. The cathodic limiting current at $\Gamma_{Ni(OH)2}$ values higher than 25 nmol cm^{-2} responded to a reactant membrane diffusion phenomenon within the nickel hydroxide film. The cathodic process for thick nickel hydroxide films was associated with the physical diffusion of the $Fe(CN)_6^{3-}$ species across the film to be reduced at the gold surface. A diffusion constant for the $Fe(CN)_6^{3-}$ species dependent on the nickel surface coverage was obtained. Although the $Fe(CN)_6^{4-}$ oxidation seemed to occur by a rapid electron-transfer process, a limiting electron-transport rate was observed at $\Gamma_{Ni(OH)2}$ values higher than 40 nmol cm^{-2} and at high electrode rotation rates (>7000 rpm).

1. Introduction

Electrodes modified by immobilization of surface-active materials that can, in principle, alternate between different valence states under the effect of external electric fields, and that are capable of mediating fast electron transfer between an electroactive substrate in the bulk solution and the electrode surface, have recently attracted great interest. Nickel hydroxide is an important electroactive material [1–3]. The good ion and electron conduction properties of nickel hydroxide films prepared by electrochemical deposition on gold have been demonstrated in previous works [4–6]. In this regard, gold electrodes modified by nickel hydroxide surface coverages below 16 nmol cm^{-2} (thickness below 4 nm) exhibit, in general, the same voltammetric response as the bare gold electrode [4–6]. However, Casella et al. [4,5] noted a decrease of about 12% in the AuO reduction charge for a nickel hydroxide surface coverage higher than 16 nmol cm^{-2}. Furthermore, for the oxidation of glucose during the negative potential scan direction, peak current values about 13% lower, as compared with the corresponding value for the bare gold electrode, have even been observed by Casella et al. [5] in the presence of a $\Gamma_{Ni(OH)2}$value of 8.7 nmol cm^{-2}. This effect of the nickel hydroxide on the electrochemical response of gold was called "screening effect" by Casella et al. [4.5]. The aim of our study was to analyze in detail the permeability limits of nickel hydroxide films deposited on gold in terms of thickness. To this end, nickel hydroxide-gold modified electrodes in the presence of the $Fe(CN)_6^{3-/4-}$ redox couple were selected. Although a qualitative study of the ferri-ferrocyanide reduction/oxidation on a Pt electrode modified with nickel-oxyhydroxide films was carried out in [7], to our knowledge, this is the first example of a systematic study of the gold/nickel hydroxide interface in the presence of the $Fe(CN)_6^{3-/4-}$ redox couple employing different nickel hydroxide film thicknesses. The present study was mainly carried out in the context of the rotating disc electrode voltammetry (RDEV) employing gold electrodes coated with nickel hydroxide surface coverages within the range 0.7 nmol $cm^{-2} < \Gamma_{Ni(OH)2} < 55$ nmol cm^{-2}. Surface resistance measurements employing gold film electrodes coated with thicker nickel films than those employed in previous work [6] were also performed here in order to observe in more detail the screening effect noted by Casella et al. [4,5]. It is expected that the present

E-mail address: rtucce@gmail.com.
[1] Mailing address: Instituto de Investigaciones Fisicoquímicas Teóricas y Aplicadas (INIFTA), Sucursal 4, Casilla de Correo 16, (1900) La Plata, Argentina.

http://dx.doi.org/10.1016/j.jelechem.2016.10.015
1572-6657/

work will shed light on the mechanism of the charge propagation across thick nickel hydroxide films deposited on gold substrates.

2. Experimental

A conventional three-electrode cell was used for the RDEV experiments. A gold rotating disc electrode (RGDE) was employed as base electrode to deposit nickel hydroxide films. A gold foil of large area was employed as counter electrode. All the potentials reported in this work are referred to the SCE. The RGDE consisted of a gold rod press-fitted with epoxy resin into a Teflon sleeve so as to leave a 1 cm^2 disc area exposed. The electrode was carefully polished with emery paper of decreasing grit size followed by alumina suspensions of size 1, 0.3 and 0.05 μm, respectively, until a mirror-like finish was obtained. Then, it was submitted to ultrasonic cleaning to remove residual abraded polishing material. In order to obtain a more specular gold surface to deposit nickel hydroxide films, a gold film about 50 nm in thickness was deposited by vacuum evaporation on the gold disc [6,8,9]. This experimental arrangement allowed one to have a base electrode of very low surface roughness to deposit nickel hydroxide films. It should be indicated that the use of an evaporated gold film as base electrode to deposit nickel hydroxide films leads to reproducible cyclic voltammetry (CV) and RDEV data. The good reproducibility can be attributed to the use of a smooth and renewable gold surface, obtained by evaporation, to deposit the nickel hydroxide film in each experiment. Nickel hydroxide was deposited on the RGDE employing the procedure described elsewhere [4], that is, after being subjected, for a different time period, to a constant potential of −0.5 V in a deoxygenated 0.5 M $Ni(NO_3)_2$ solution, the RGDE was transferred to a deoxygenated 0.2 M Na(OH) solution and cycled between −0.5 V and 0.6 V (vs. SCE) at 10 mV s^{-1} until a stable voltammogram was achieved (150 cycles). This procedure allows one to obtain different nickel hydroxide surface coverages ($\Gamma_{Ni(OH)2}$). The surface coverage of the different Au/$Ni(OH)_2$ modified electrodes was estimated from the voltammetric oxidation (or reduction) charge ($Q_{Ni(OH)2}$) evaluated in the supporting electrolyte solution (0.2 M NaOH) by using the equation $\Gamma_{Ni(OH)2} = Q_{Ni(OH)2} / nFA$, where $Q_{Ni(OH)2}$ is the anodic (or cathodic) voltammetric charge corresponding to the oxidation (or reduction) process, assuming that all the nickel redox sites are electroactive on the voltammetric time scale; F is the Faraday's constant; A is the geometric surface area of the gold electrode; and n is the number of electrons transferred in the Ni(II) ⇔ Ni(III) oxidation (reduction) reaction. Nickel hydroxide surface coverages within the range 0.7 nmol cm^{-2} to 55 nmol cm^{-2} were obtained. Potentiodynamic and steady-state experiments were performed with these nickel hydroxide-gold modified electrodes in contact with a 0.2 M NaOH + 5×10^{-3} M $Fe(CN)_6^{3-/4-}$ solution. In some experiments, Na(OH) and $Fe(CN)_6^{3-/4-}$ concentrations were independently varied. All measurements were performed employing electrolyte solutions previously deoxygenated by N_2 bubbling for 5 h. The reduction of the oxygen content in the electrolyte solution was necessary in order to avoid the interference of the O_2 reduction process in the CV and RDEV responses. Both types of experiments were performed using a measurement system comprising a PAR model 175 universal programmer and a PAR model 173 potentiostat-galvanostat. A Philips model 8134 X-Y1-Y2 recorder was used to record potentiodynamic and stationary current-potential curves. The electrode rotation rate Ω was controlled with homemade equipment that allowed one to select a constant Ω value in the range 50 rev $min^{-1} < \Omega <$ 9000 rev min^{-1}. In some cases, higher electrode rotation speed values (>10,000 rev min^{-1}) were employed. This was controlled with a digital photo tachometer (Power Instruments model 891). Scanning electron microscopy (SEM) observations were carried out with a Phillips SEM 505 scanning electron microscope.

Some surface resistance (SR) measurements [6] were also performed. To this end, three gold films were prepared by vacuum evaporation, as was previously described [6]. The relationship between the length, l, and the width, w, ($G = l / w$) of these gold film electrodes was 25. The electrode area was 1 cm^2. Each gold film electrode was conditioned electrochemically by cycling the potential between −0.5 V and 0.6 V for 150 cycles at a scan rate of 10 mV s^{-1} in a deoxygenated 0.2 M Na(OH) solution. Nickel hydroxide was deposited on the gold film electrodes employing the procedure described above [4]. Each one of the three gold films was coated with a different nickel surface coverage, $\Gamma_{Ni(OH)2}$ = 25, 34 and 41 nmol cm^{-2}, respectively, and SR and voltammetric responses were simultaneously recorded only in the presence of the supporting electrolyte 0.2 M Na(OH).

AR grade chemicals were employed throughout. $Ni(NO_3)_2$ (Fluka) was employed. $K_3Fe(CN)_6$, $K_4Fe(CN)_6$ and NaOH (Merck) were used without purification. Solutions were prepared with water purified using a Millipore Milli-Q system.

3. Results and discussion

3.1. Cyclic voltammetry and SR measurements

The voltammetric response of a gold electrode modified with different nickel hydroxide surface coverages ($\Gamma_{Ni(OH)2}$) in the presence of a 0.2 M Na(OH) solution is shown in Fig. 1. This voltammetric response is the weighted sum of the activities of gold and nickel hydroxide. Two redox transitions are observed: a1/c1, which is related to gold–oxide formation and reformation of Au°, and a2/c2, which is due to the Ni(II)/Ni(III) system [10,11]. The shape of the Ni(II)/Ni(III) transition (i.e., peak separation, peak current ratios and peak potentials) is influenced by the $\Gamma_{Ni(OH)2}$ value. Although the stabilized voltammetric responses obtained after prolonged potential cycling (around 150 potential cycles at 10 mV s^{-1}) are shown in Fig. 1, it is well-known that during continuous electrochemical cycling in alkaline solutions, the Au/$Ni(OH)_2$ electrode undergoes profound physical and/or structural changes [4,5]. In this regard, we observe that the voltammetric response drastically changes with the number of potential cycles. As has been reported [4,5,11], nickel hydroxide can exist in at least two different crystallographic forms such as α-$Ni(OH)_2$ and β-$Ni(OH)_2$. The α-$Ni(OH)_2$ is known to be unstable in alkaline medium and converts slowly and irreversibly to β-$Ni(OH)_2$. In addition, the oxidation of nickel hydroxide gives other two varieties of oxyhydroxides, β and γ. Thus, the surface concentration of nickel oxyhydroxide increases, and the gold film electrode also undergoes surface reconstruction during multiple potential cycling. However, as was indicated, in the present work only stabilized voltammetric responses of the Au/$Ni(OH)_2$ electrode are analyzed.

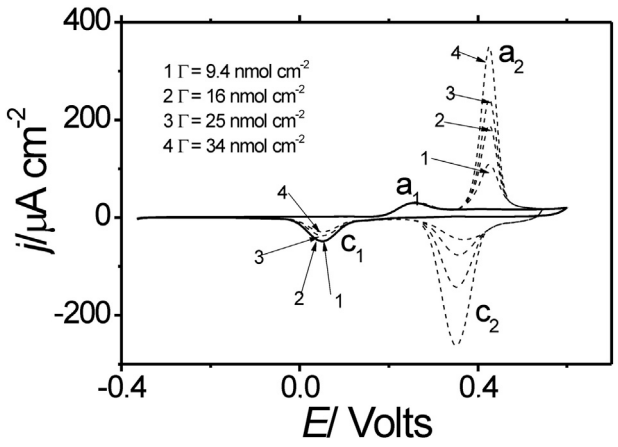

Fig. 1. (Dashed line) Voltammetric response of a gold electrode modified with different nickel hydroxide surface coverages. $\Gamma_{Ni(OH)2}$ values are indicated in the figure. (Solid line) Voltammetric response of the bare gold electrode. Electrolyte: 0.2 M Na(OH). Scan rate: 0.01 V s^{-1}. Numbers and arrows indicate voltammetric responses corresponding to different $\Gamma_{Ni(OH)2}$ values.

The $Ni(OH)_2$ and NiOOH species have been considered good electronic and ion conductors with a structure of poor or not barrier character [4,5]. In this regard, peak currents and potentials related to gold–oxide formation and reduction (a1/c1) in the presence of the nickel hydroxide film are virtually identical to those observed for the bare gold electrode within the nickel surface coverage range 0.7 nmol cm^{-2} < $\Gamma_{Ni(OH)2}$ < 25 nmol cm^{-2} (Fig. 1). However, a decrease of the charge under the wave c1 is observed for $\Gamma_{Ni(OH)2}$ values higher than 25 nmol cm^{-2} (see arrows on peak c1 in Fig. 1). This effect was previously reported by Casella at al. [4,5]. Thick enough nickel hydroxide films seem to cause an attenuation or screening effect in the gold reduction process. This screening effect is also observed in the surface resistance (SR) response of a gold film electrode coated with thick enough nickel hydroxide films (Fig. 2) [6]. As can be seen from Fig. 2, the SR of a gold film electrode modified by nickel hydroxide surface coverages higher than 25 nmol cm^{-2} always remains higher than that corresponding to the bare gold electrode during the AuO reduction process in going from 0.2 V to −0.1 V. Also, the higher the nickel surface coverage is, the higher the SR becomes at each potential for the AuO reduction process as compared with the SR of the bare gold electrode. As was indicated, correspondingly, the c1 peak current decreases within the same potential region. These different SR responses seem to confirm the existence of a screening or blocking effect at high nickel hydroxide surface coverages, where the AuO reduction is not complete within the potential region corresponding to peak c1.

In order to analyze in more detail this screening effect, voltammetric measurements were performed with the gold electrode coated with nickel hydroxide films within the range 0.7 nmol cm^{-2} < $\Gamma_{Ni(OH)2}$ < 41 nmol cm^{-2} in contact with a solution containing the $Fe(CN)_6^{3-/4-}$ redox couple. As for the gold-reduction process, within the nickel hydroxide surface coverage range comprised between 0.7 nmol cm^{-2} and 16 nmol cm^{-2}, no attenuation effect on the current waves corresponding to the ferri-ferrocyanide reduction-oxidation processes was observed. Voltammograms for nickel hydroxide surface coverage within the range 3.1 nmol cm^{-2} < $\Gamma_{Ni(OH)2}$ < 16 nmol cm^{-2} are shown in Fig. 3. As can be seen, the current waves corresponding to the ferri-ferrocyanide reduction-oxidation processes on these different nickel hydroxide-gold modified electrodes are virtually identical between them, and also with that observed on the bare gold electrode (onset at E = 0.15 V, not shown) [12].

However, a progressive attenuation of the current wave corresponding to the ferricyanide reduction process is observed for $\Gamma_{Ni(OH)2}$ higher than 25 nmol cm^{-2} within the potential range −0.1 < E < 0.25 V (Fig. 4). This attenuation seems to be consistent with the screening effect

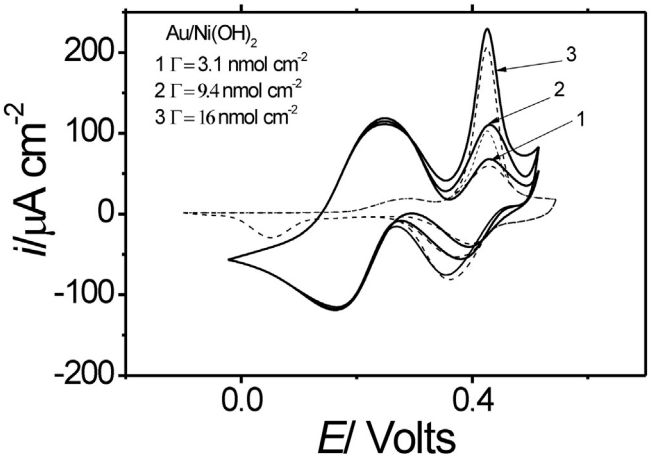

Fig. 3. (Dashed line) Voltammetric response of a gold electrode modified with different nickel hydroxide surface coverages in contact with a 0.2 M Na(OH) solution. (Solid line) Voltammetric response of the same gold modified electrodes in contact with a 0.2 M Na(OH) + 5×10^{-3} M $Fe(CN)_6^{3-/4-}$ solution. $\Gamma_{Ni(OH)2}$ values are indicated in the figure. Scan rate: 0.01 V s^{-1}.

observed for the above-described AuO reduction process. At this point, it should be indicated that when voltammetric responses of the bare gold electrode and the nickel hydroxide-gold modified electrode are compared in the presence of some organic compounds, such as glucose, it is also observed that while the current in going towards the positive direction scan remains the same for both electrodes, the current in going towards the negative direction for the modified electrodes is lower than that of the bare gold electrode [4]. Also, for the oxidation of glucose during the negative potential scan direction, peak current values about 13% lower have been observed in the presence of a $\Gamma_{Ni(OH)2}$ value of 8.7 nmol cm^{-2}, as compared with the corresponding value for the bare gold electrode [5]. Then, in order to obtain a more clear understanding about this screening effect of the nickel hydroxide on the electrochemical response of a gold electrode, RDEV measurements with a gold electrode coated with nickel hydroxide films of different thicknesses in the presence of a $Fe(CN)_6^{3-/4-}$ solution were performed. In the context of this technique, it is expected to detect permeability changes of a nickel hydroxide film as a function of its thickness, and then, to establish the limiting thickness at which a nickel

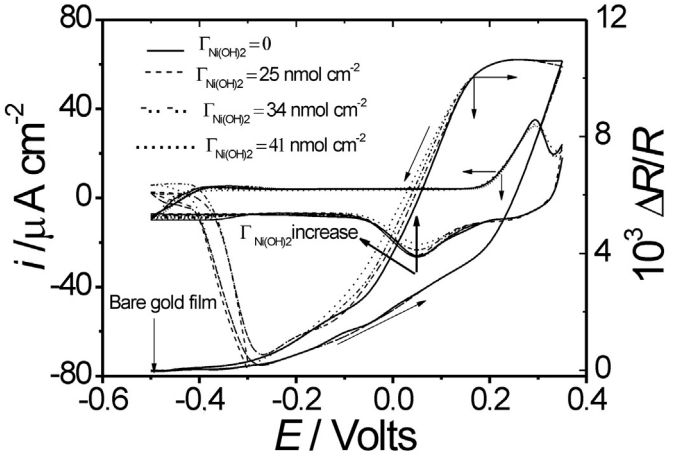

Fig. 2. Simultaneous voltammetric and SR responses of a gold film electrode modified with different nickel hydroxide surface coverages within the potential range −0.5 V < E < 0.35 V. The $\Gamma_{Ni(OH)2}$ values are indicated in the figure. The solid line corresponds to the bare gold electrode responses. Electrolyte: 0.2 M Na(OH). Scan rate: 0.01 V s^{-1}.

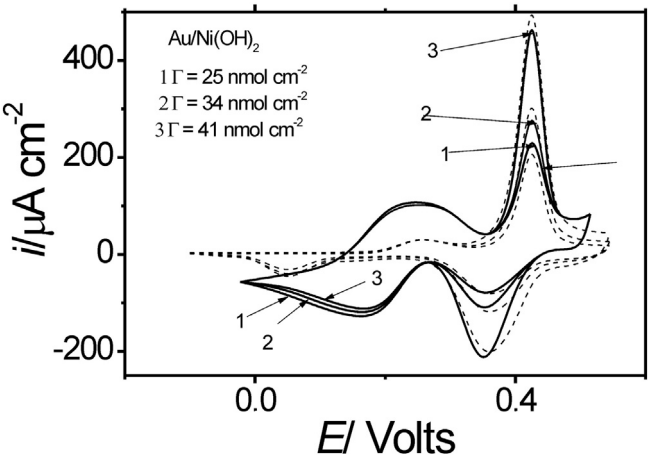

Fig. 4. (Dashed line) Voltammetric response of a gold electrode modified with different nickel hydroxide surface coverages in contact with a 0.2 M Na(OH) solution. (Solid line) Voltammetric response of the same gold modified electrodes in contact with a 0.2 M Na(OH) + 5×10^{-3} M $Fe(CN)_6^{3-/4-}$ solution. $\Gamma_{Ni(OH)2}$ values are indicated in the figure. Scan rate: 0.01 V s^{-1}.

hydroxide film is able to act as an effective barrier to restrict the charge transport process at the gold surface substrate.

3.2. RDEV experiments

Steady-state current-potential (*I-E*) curves, at different electrode rotation rates, 0 rpm < Ω < 5000 rpm, for the bare gold electrode and a nickel hydroxide-gold modified electrode with a surface coverage $\Gamma_{Ni(OH)2} = 25$ nmol cm^{-2} are compared in Fig. 5. The same *I-E* dependences for the bare gold electrode and the gold electrode modified with a nickel hydroxide surface coverage of $\Gamma_{Ni(OH)2} = 9.4$ nmol cm^{-2} are shown in the inset of Fig. 5. In both cases, diffusion-limited currents at $E > 0.25$ V (vs. SCE) for the $Fe(CN)_6^{4-}$ oxidation and at $E < 0.0$ V (vs. SCE) for the $Fe(CN)_6^{3-}$ reduction are observed. However, while *I-E* dependences for the bare gold electrode and nickel hydroxide-gold modified electrodes with surface coverages within the range 0.7 nmol cm^{-2} < $\Gamma_{Ni(OH)2}$ < 16 nmol cm^{-2} are the same (inset in Fig. 5), an attenuation of the cathodic limiting current at each Ω value for nickel hydroxide modified electrodes with surface coverages higher than 16 nmol cm^{-2}, as compared with that of the bare gold electrode, is observed. Although the cathodic limiting current decreases as $\Gamma_{Ni(OH)2}$ increases beyond 25 nmol cm^{-2}, the anodic one remains independent of $\Gamma_{Ni(OH)2}$. These features seem to be consistent with the potentiodynamic records shown in Fig. 4 for the ferricyanide reduction and ferrocyanide oxidation, respectively. The anodic limiting current ($I_{Lim,a}$) for both the bare gold electrode and the different modified electrodes follows the Levich dependence [13] (inset in Fig. 6):

$$I_{Lim,a} = 0.62\, nFA\, D^{2/3} \nu^{-1/6}\, \Omega^{1/2}\, C_o \quad (1)$$

In Eq. (1) *F* is the Faraday's constant, *A* is the geometric surface area of the gold electrode, and *n* is the number of electrons transferred in the $Fe(CN)_6^{-4} \rightarrow Fe(CN)_6^{-3}$ reaction. C_o and *D* are the concentration and the diffusion coefficients, respectively, of the redox species in the solution, and ν is the kinematic viscosity of the solution.

The cathodic limiting current as a function of $\Omega^{1/2}$ for nickel hydroxide surface coverages higher than 25 nmol cm^{-2} is shown in Fig. 6. The limiting current exhibits a negative departure from the Levich equation [13]. Besides, the higher the nickel hydroxide surface coverage, the more pronounced the cathodic limiting current curvature. Then, concerning RDEV experiments, two regimes of $\Gamma_{Ni(OH)2}$ values are observed: (*i*) gold electrodes modified with nickel hydroxide surface coverages within the range 0.7 nmol cm^{-2}–<$\Gamma_{Ni(OH)2}$ < 16 nmol cm^{-2} are good ion and electron conductors for the oxidation of ferrocyanide and the reduction of ferricyanide ions. Steady-state current-potential (*I-E*) curves for these modified electrodes are the same as that for the bare gold electrode and then, the Levich dependence is observed for both the anodic and cathodic processes (inset in Fig. 6). (*ii*) Although gold electrodes modified with nickel hydroxide surface coverages higher than 25 nmol cm^{-2} exhibit an anodic limiting current equal to that of the bare gold electrode, cathodic limiting currents are lower than that corresponding to the bare gold electrode and they do not follow the Levich relationship. Then, we assume that the gradual deviation of the cathodic limiting current from the Levich dependence at high enough surface coverage is due to a restriction for the ferricyanide transport through the nickel hydroxide film to be discharged at the gold surface. Then, Eq. (2), developed for a reactant membrane diffusion phenomenon in RDEV [13], was employed in this work to interpret the attenuation of the cathodic plateau with the increase of the nickel surface coverage:

$$I_{Lim,c}^{-1} = \Gamma_{Ni(OH)2}\,(nFA\, c_o \kappa D_{film}\, C_o)^{-1} + \left(0.62\, nFA\, D^{2/3} \nu^{-1/6}\, \Omega^{1/2}\, C_o\right)^{-1} \quad (2)$$

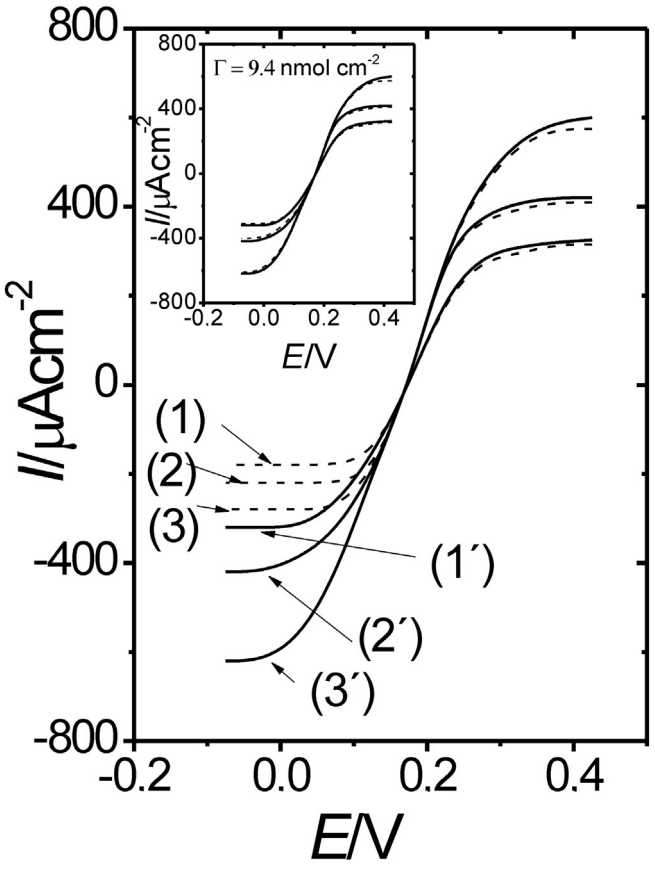

Fig. 5. (- - - -) Steady-state current-potential (*I-E*) curves for the nickel hydroxide-gold modified electrode and (—) the bare gold electrode in contact with a 0.2 M Na(OH) + 5×10^{-3} M $Fe(CN)_6^{3-/4-}$ solution. Rotation rates, Ω: (1,1′) 700 rpm, (2,2′) 1200 rpm and (3,3′) 2600 rpm. $\Gamma_{Ni(OH)2} = 25$ nmol cm^{-2}. Numbers with a quotation mark correspond to the naked gold electrode. Inset: (- - - -) steady-state current-potential (*I-E*) curves for a nickel hydroxide-gold modified electrode ($\Gamma_{Ni(OH)2} = 9.4$ nmol cm^{-2}) and (—) the bare gold electrode. The same electrolyte solution and electrode rotation rates as in Fig. 5.

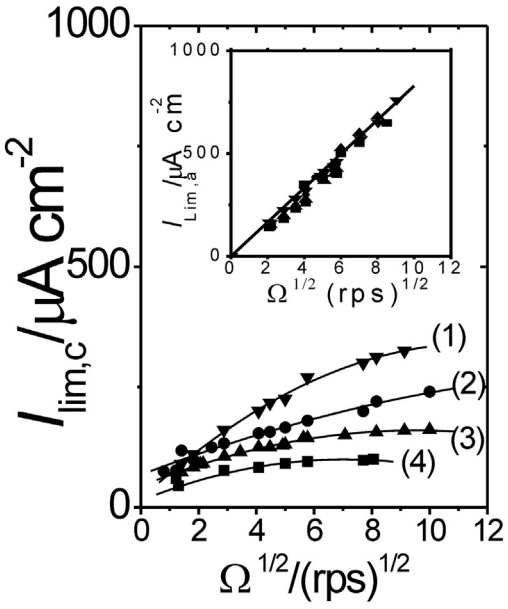

Fig. 6. Cathodic limiting currents as a function of $\Omega^{1/2}$ for different nickel hydroxide surface coverages: (▼) 25 nmol cm^{-2}; (●) 34 nmol cm^{-2}; (▲) 41 nmol cm^{-2}; (■) 55 nmol cm^{-2} Solution: 0.2 M Na(OH) + 5×10^{-3} M $Fe(CN)_6^{3-/4-}$. Inset: anodic limiting currents as a function of $\Omega^{1/2}$ for the same nickel hydroxide surface coverages indicated in Fig. 6.

The existence of a film of limited permeability covering reacting metallic surfaces is considered in the first term of Eq. (2). This film may slow down the mass transfer rate of diffusing species towards the electrode surfaces [13]. On the assumption that thick nickel hydroxide films covering the gold surface are uniform and homogeneous, the film thickness, ϕ_{film}, can be expressed as $\Gamma_{Ni(OH)2} / c_o$ in the first term of Eq. (2). The parameter c_o is the total volumetric concentration of redox sites in the nickel film. A c_o value of 40×10^{-3} mol cm^{-3} for nickel hydroxide films is reported in [7]. Besides, Eq. (2) assumes that the electroactive species dissolves into the film deposited on the base electrode material with a partition equilibrium coefficient $\kappa = c_{film} / C_o$ at the film|solution interface, where c_{film} and C_o are the concentrations of the redox species in the film and in the solution, respectively. D_{film} is the diffusion coefficient of the electroactive species ($Fe(CN)_6^{3-}$) in the film. The reciprocal currents (Eq. (2)) are usually employed for processes occurring in series (Eq. (2)). While the second term in Eq. (2) refers to the limiting diffusion flux on the metallic surface free of the screening film, the first one represents the limiting flux when the entire concentration gradient is located within the film of low permeability. The interest of using reciprocal values in Eq. (2) is that an experimental plot of $I_{Lim,c}^{-1}$vs. $\Omega^{-1/2}$ must be a straight line parallel to the Levich linear variation, which passes through the origin. The ordinate value of the intercept of this straight line at $\Omega^{-1/2} = 0$ ($\Omega \to \infty$) is the first term of Eq. (2) and hence provides the film permeability D_{film}/ϕ_{film} [13]. At this point, it should be indicated that deviations of experimental limiting currents from the Levich plot as shown in Fig. 6 were also observed for the reduction of ferricyanide ion on nickel electrodes [14], which was attributed to a passivation effect of the nickel hydroxide generated on the nickel surface. However, the more pronounced deviation of the cathodic limiting current from the Levich dependence as the nickel hydroxide surface coverage increases beyond 25 nmol cm^{-2} shown in Fig. 6 and the absence of this effect for thin nickel hydroxide films lead us to associate this phenomenon with a progressive restriction for ferricyanide ion transport through the nickel hydroxide film to be reduced at the gold surface. As can be seen from Fig. 7, experimental $I_{Lim,c}^{-1}$ vs. $\Omega^{-1/2}$ representations for different $\Gamma_{Ni(OH)2}$ values give linear diagrams with the same slope but different intercepts on the ordinate axis. By using a linear regression method, we determined the intercept at $\Omega \to \infty$ from the plots shown in Fig. 7 and then, κD_{film} was extracted using the first term of Eq. (2). This parameter should represent a measure of the diffusion rate of $Fe(CN)_6^{3-}$ species incorporated into the nickel hydroxide film.

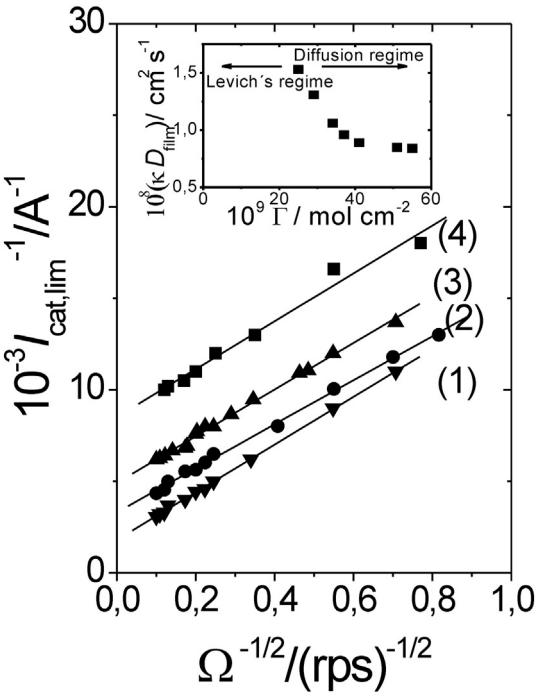

Fig. 7. Koutecky-Levich plots ($I_{cat,lim}^{-1}$ vs. $\Omega^{-1/2}$) for the cathodic plateau. Different nickel hydroxide charge values: (1) (▼) 25 nmol cm^{-2}; (2) (●) 34 nmol cm^{-2}; (3) (▲) 41 nmol cm^{-2}; (4) (■) 55 nmol cm^{-2}. Solution: 0.2 M Na(OH) + 5×10^{-3} M $Fe(CN)_6^{3-/4-}$. Inset: diffusion constant (κD_{film}) extracted from Eq. (2) as a function of the nickel hydroxide surface coverage $\Gamma_{Ni(OH)2}$. The same solution indicated in Fig. 7.

As can be seen from Table 1 and the inset in Fig. 7, (κD_{film}) decreases when the $\Gamma_{Ni(OH)2}$ value increases. However, after a certain $\Gamma_{Ni(OH)2}$ value ($\Gamma_{Ni(OH)2} > 40$ nmol cm^{-2}), the (κD_{film}) value becomes relatively independent of $\Gamma_{Ni(OH)2}$. Then, the diffusion constant estimated for $\Gamma_{Ni(OH)2}$ values higher than 40 nmol cm^{-2} should represent a true permeation rate through nickel hydroxide deposited on gold (see below). The (κD_{film}) parameter contains the diffusion rate (D_{film}) of $Fe(CN)_6^{3-}$ species that penetrate through the nickel hydroxide film and the partition equilibrium coefficient, κ, which should be between 0 and 1.

The decrease of κD_{film} with the increase of the nickel hydroxide film thickness could be explained by assuming that external supporting electrolyte contacting films could be incorporated into the film matrix. This internal electrolyte can play an important role in the conduction process, making the charge propagation within the film easier. It should be expected that κ is related to the content of electrolyte in the nickel hydroxide film. In other words, the decrease of (κD_{film}) could be attributed to a decrease in the permeability of the nickel hydroxide film, as a result of the formation of a more compact layer as the film thickness increases. That is, the denser structures as the film thickness increases would restrain the content of the electrolyte in the film and also the physical diffusion process of species through it. On the contrary, in the open structures exhibited by low surface coverages there would be enough room for the electrolyte solution to be incorporated in the void space of the hydroxide nickel film. Within the framework of the assumption of a different degree of hydration with increasing film thickness, it would be expected that an increase in the solute (ferricyanide) or supporting electrolyte (Na(OH)) concentration in solution will cause an increase in the solute or supporting electrolyte concentration within the spaces in the hydrated structures of thin nickel hydroxide films and then, a decrease in the resistance in the transport process through them. Thus, an increase in the (κD_{film}) transport parameter for nickel hydroxide films should be expected for relatively low $\Gamma_{Ni(OH)2}$ values as the concentration of the external solution (ferricyanide or Na(OH)) increases. On the contrary, compact structures would hinder the incorporation of electrolyte solution into the hydroxide nickel phase and then, the transport rate across a thick film would be less sensitive to concentration changes of species in solution. In order to verify this assumption, experiments were carried out employing contacting solutions with two different nickel hydroxide surface coverages ($\Gamma_{Ni(OH)2} = 29$ nmol cm^{-2} and 51 nmol cm^{-2}), where the concentration of the external redox couple and that of Na(OH) were changed. With regard to the redox couple concentration, in agreement with Eq. (2), at constant $\Gamma_{Ni(OH)2}$, both the slope and intercept at $\Omega \to \infty$ of

Table 1
Dependence of the (κD_{film}) diffusion constant on the nickel hydroxide voltammetric charge value (or $\Gamma_{Ni(OH)2}$).

$10^9 \Gamma_{Ni(OH)2}$/mol cm^{-2}	$10^8 \kappa D_{film}$/cm^{-2} s^{-1}
25	1.53
29	1.31
34	1.06
37	0.96
41	0.89
51	0.85
55	0.84

$\Gamma_{Ni(OH)2}$ ($= Q / nFA$) was calculated from the voltammetric charge (Q) under the oxidation peak of the voltammogram in 0.2 M NaOH.
A is the geometric surface area of the gold electrode and n is the number of electrons transferred in the reaction Ni(II) ⇔ Ni(III). Electrolyte: 0.2 M NaOH + 5×10^{-3} M $Fe(CN)_6^{3-/4-}$.

Table 2
Dependence of the diffusion constant (κD_{film}) on the external redox couple concentration.

$10^9\ \Gamma_{Ni(OH)2}$/mol cm^{-2}	$10^3\ C_o$/mol L^{-1}	$10^8\ \kappa D_{film}$/cm^2 s^{-1}
29	5	1.31
	8	1.42
	12	1.49
51	5	0.85
	8	0.83
	12	0.86

experimental $I_{cath,I}^{-1}$ versus $\Omega^{-1/2}$ representations should decrease with increasing C_o (ferro-ferricyanide species). Then, again, from the intercept on the ordinate axis for the different C_o values, (κD_{film}) values as function of C_o, for both film thicknesses, were extracted. As can be seen from Table 2, while for $\Gamma_{Ni(OH)2} = 51$ nmol cm^{-2} the (κD_{film}) value remains at $(0.83 \pm 0.02) \times 10^{-8}$ cm^2 s^{-1} when increasing C_o from 5×10^{-3} to 12×10^{-3} M, this value for the 29 nmol cm^{-2} film increases systematically with C_o. Table 3 shows the effect of the increase in Na(OH) concentration while the redox species concentration remains constant, for the 29 nmol cm^{-2} and 51 nmol cm^{-2} nickel hydroxide surface coverages. As can be seen from Table 3, again, while the κD_{film} value increases as the Na(OH) concentration for the 29 nmol cm^{-2} film increases, it remains approximately constant for the thicker nickel hydroxide film ($\Gamma_{Ni(OH)2} = 51$ nmol cm^{-2}). This finding seems to indicate that the supporting electrolyte (OH^- and Na^+ species) incorporated into thin nickel hydroxide films also increases the charge propagation rate. As probably thick films do not allow enough electrolyte incorporation (electroactive species or Na(OH)) into the film structure, the parameter κD_{film} remains independent of the external electrolyte concentration (Tables 2 and 3). With regard to the effect of the supporting electrolyte (Na(OH)) on the transport properties inside the nickel hydroxide film, besides the OH^- contribution to the film conductivity, as κD_{film} is evaluated for the reduction process ($Fe^{III}(CN)_6^{-3} + e^- \rightarrow Fe^{II}(CN)_6^{-4}$), it is possible that Na^+ acts as compensating ion of the negative charges reducing interactions between them, which should facilitate the transport of electroactive species. Our assumption about different degrees of permeation dependent on the nickel hydroxide coverage seems to be confirmed by SEM images. Fig. 8 shows SEM micrographs of the 29, 40, 51 nmol cm^{-2} nickel hydroxide films deposited on the gold rotating disc electrode previously covered with a specular gold film (thickness: 50 nm) obtained by high vacuum evaporation (see Experimental section [8,9]). As can be seen, while the 29 nmol cm^{-2} film shows a rather dispersed porous structure, the 40, 51 nmol cm^{-2} nickel hydroxide films exhibit more compact and smooth structures. The ellipsometric study of nickel hydroxide electrodes formed by ex situ chemical precipitation reported in [15] also shows the formation of a compact structure at high thickness values as compared with the hydrated structure formed at lower charge values.

The constant κD_{film} value of about 8.9×10^{-9} cm^2 s^{-1} for the diffusion rate at the reduced state of thick nickel hydroxide films (independent of the external solution) can be compared with diffusion coefficient values of electroinactive species, such as protons ($Ni(OH)_2 \leftrightarrow NiO(OH) + H^+ + e^-$). Some authors assume that the proton diffusion across nickel hydroxide occurs by a hopping mechanism, where the proton hops from one oxyhydroxide site to another [16]. The diffusion coefficient of hydrogen in pure NiOOH is found to be

Table 3
Dependence of the diffusion constant (κD_{film}) on the Na(OH) concentration.

$10^9\ \Gamma_{Ni(OH)2}$/mol cm^{-2}	$10^3\ C_o$/mol L^{-1}	[Na(OH)]/mol L^{-1}	$10^8\ \kappa D_{film}$/cm^2 s^{-1}
29	5	0.2	1.31
		1.3	1.47
		2	1.55
51	5	0.2	0.85
		1.3	0.87
		2	0.87

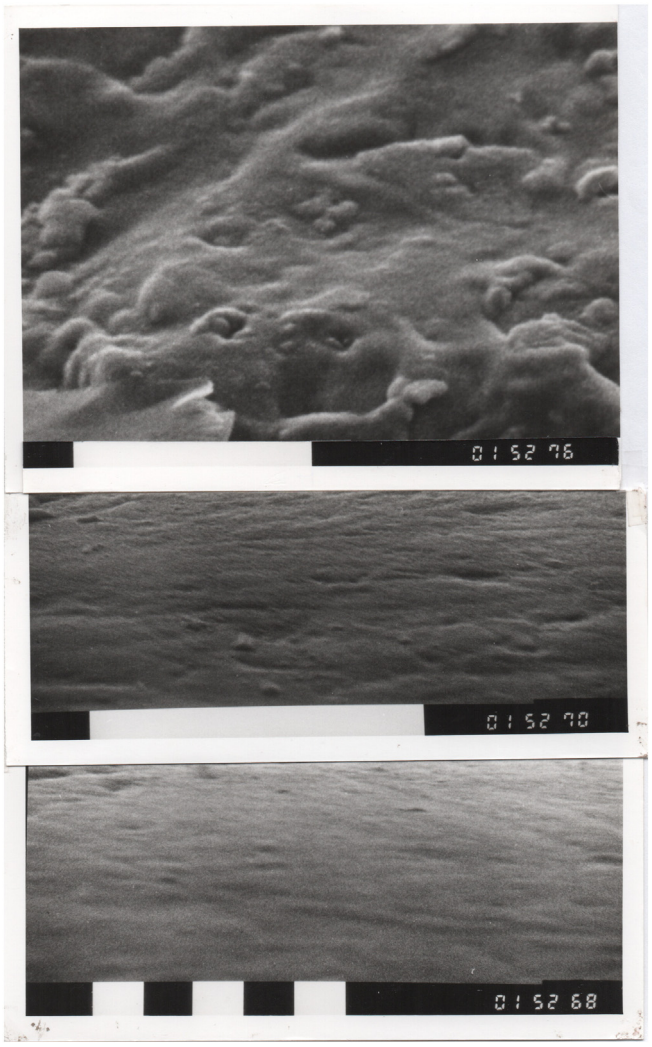

Fig. 8. SEM images of nickel hydroxide films deposited on the RDE previously covered with an evaporated gold film of 50 nm thickness. Upper image ($\Gamma_{Ni(OH)2} = 29$ nmol cm^{-2}); middle image ($\Gamma_{Ni(OH)2} = 41$ nmol cm^{-2}); lower image ($\Gamma_{Ni(OH)2} = 51$ nmol cm^{-2}). The white sticks below are (upper image) 10 μm × 7000; (middle image) 12 μm × 7000; (lower image) 1 μm × 10,000.

3.4×10^{-8} cm^2 s^{-1} and as the state of charge decreases, the concentration of NiOOH decreases and hence, the diffusion coefficient decreases [17–19]. In this regard, the diffusion coefficient of protons is found to decrease from 3.4×10^{-8} cm^2 s^{-1} to 3.7×10^{-9} cm^2 s^{-1} as the electrode changes from fully charged to 30% state of charge [20]. The diffusion coefficient for hydrogen in pure $Ni(OH)_2$ is found to be 6.4×10^{-11} cm^2 s^{-1} [16]. In this regard, the proton diffusion coefficient decreases almost three orders of magnitude in going from the oxidized (NiOOH) to the reduced ($Ni(OH)_2$) state of nickel hydroxide. A lower diffusion rate of protons across $Ni(OH)_2$ species as compared with that across NiOOH species seems to be consistent with a lower permeation rate of electroactive species (ferricyanide) at the reduced state of thick nickel hydroxide films as compared with that at the oxidized state (ferrocyanide). Our κD_{film} value seems to be of the same order of magnitude as the proton diffusion coefficient value at low state of charge. Differences can be explained in terms of either different ion charges (positive for proton and negative for $Fe(CN)_6^{3-}$ and OH^-) or different transport mechanisms for these species.

As was indicated, the anodic limiting current for $Fe(CN)_6^{4-}$ oxidation ($E > 0.25$ V) depends linearly on $\Omega^{1/2}$ ($0 < \Omega < 5000$ rpm) and it is independent of the film thickness (inset in Fig. 6). This behavior seems to be

consistent with the good conducting properties predicted for nickel hydroxide [4,5]. Although the linear dependence shown in the inset of Fig.6 remains up to a surface coverage of about 35 nmol cm^{-2}, when thicker nickel hydroxide films ($\Gamma_{Ni(OH)2} > 40$ nmol cm^{-2}) and a high electrode rotation rate ($\Omega > 7000$ rpm) are employed, the anodic limiting current reaches a constant value (black circles in Fig. 9). This constant anodic current cannot be observed at a surface coverage lower than 35 nmol cm^{-2}. The existence of a constant current I_{const} (1022 μA) in a thick nickel hydroxide film at high electrode rotation rates can be explained in the following way. As one increases the flux of electroactive species (Ω increase) from the bulk solution, then if the flux exceeds the supply of charge from the gold electrode through the nickel hydroxide film to the electrolyte interface, the rate-limiting step will shift from the limiting transport of the electroactive species to the limiting transport of the charge through the nickel hydroxide film. A constant current may also be observed for lower surface coverage values, but it should occur at extremely high electrode rotation rates ($\Omega > 9000$ rpm). However, at such high angular speed of the rotating disc electrode, the flux into the solution would no longer be laminar, so that the proportionality between current and $\Omega^{1/2}$ should not be expected. Despite this consideration, the value of the constant current ($I_{const} = 1022$ μA) reached for $\Omega > 7000$ rpm for a thick film is reproducible and independent of the redox solute concentration (Fig. 9). This fact should indicate the existence of a restriction in the electron transport process across thick nickel hydroxide films at high electrode rotation rates.

4. Conclusion

RDEV experiments carried out with nickel hydroxide-gold modified electrodes in the presence of an electroactive solution containing $Fe(CN)_6^{3-/4-}$ species reveal the existence of different charge transport processes dependent on the nickel hydroxide surface coverage. The ferri-ferrocyanide reduction-oxidation processes at a gold electrode modified with nickel surface coverages within the range 0.7 nmol cm^{-2}–$<\Gamma_{Ni(OH)2} < 16$ nmol cm^{-2} are virtually identical to those observed for the bare gold electrode. This fact shows the good electron and ion conductivities of relatively low nickel hydroxide surface coverages. Nickel hydroxide surface coverages within the range 25 nmol cm^{-2}–$<\Gamma_{Ni(OH)2} < 35$ nmol cm^{-2} are not so good ion conductors to allow the easy transport of ferricyanide ions to be reduced at the gold surface. The diffusion constant (κD_{film}) for ferricyanide ion transport progressively decreases from 1.53×10^{-8} cm^2 s^{-1} to 1.2×10^{-8} cm^2 s^{-1} as $\Gamma_{Ni(OH)2}$ increases from 25 nmol cm^{-2} to 35 nmol cm^{-2}. However, these nickel hydroxide films even have enough permeability to incorporate the electrolyte into their structures, giving rise to high enough transport rates through them. In this regard, the parameter κD_{film}, within the coverage range 25 nmol cm^{-2} to 35 nmol cm^{-2}, depends on both $Fe(CN)_6^{3/-4}$ and Na(OH) concentration. However, nickel hydroxide surface coverages higher than 40 nmol cm^{-2} could not incorporate the external electrolyte into their structures and then, the transport process of species across them becomes slow. The diffusion constant value of $\kappa D_{film} = 8.90 \times 10^{-9}$ cm^2 s^{-1}, obtained for nickel hydroxide films within the thickness range comprised between 40 nmol cm^{-2} and 55 nmol cm^{-2}, is independent of both $Fe(CN)_6^{3/-4}$ and Na(OH) concentration. Nickel hydroxide surface coverages within the range 40 nmol $cm^{-2} < \Gamma_{Ni(OH)2} < 55$ nmol cm^{-2} and at high electrode rotation rates (>7000 rpm) also show a limiting electron transport rate for the ferrocyanide oxidation process.

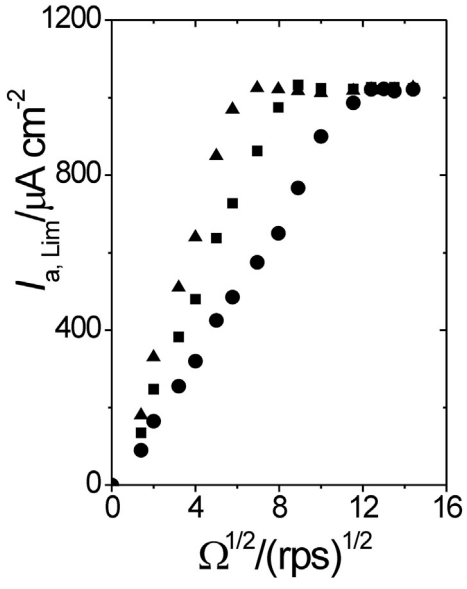

Fig. 9. Levich representations ($I_{a,lim}$ vs. $\Omega^{1/2}$) for the anodic plateau at different redox couple concentrations in solution. Solutions: 0.2 M Na(OH) + x M $Fe(CN)_6^{3-/4-}$, where x (●) 5×10^{-3} M; (■) 8.0×10^{-3} M, and (▲) 10×10^{-3} M. $\Gamma_{Ni(OH)2} = 40$ nmol cm^{-2}.

Conflict of interest

The author declares that he has not conflict of interest.

Acknowledgements

The author gratefully acknowledges the Consejo Nacional de Investigaciones Científicas y Técnicas (CONICET) and also the Facultad de Ciencias Exactas, National University of La Plata (UNLP).

References

[1] S. Madji, A. Jabbari, H. Heli, A.A. Moosavi-Movahed, Electrocatalytic oxidation of some amino acids on a nickel-curcumin complex modified glassy carbon electrode, Electrochim. Acta 52 (2007) 4622–4629.
[2] S. Madji, A. Jabbari, H. Heli, A study of the electrocatalytic oxidation of aspirin on a nickel hydroxide-modified nickel electrode, J. Solid State Electrochem. 11 (2007) 601–607.
[3] M. Jafarian, M.G. Mahjani, H. Heli, F. Gobal, M. Heydarpoor, Electrocatalytic oxidation of methane at nickel hydroxide modified nickel electrode in alkaline solution, Electrochem. Commun. 5 (2003) 184–188.
[4] I.G. Casella, M.R. Guascito, M.G. Sannazzaro, Voltammetric and XPS investigations of nickel hydroxide electrochemically dispered on gold surface electrodes, J. Electroanal. Chem. 462 (1999) 202–210.
[5] I.G. Casella, M.R. Guascito, T.M.R.I. Cataldi, Electrocatalysis and amperometric detection of alditols and sugars at a gold-nickel composite electrode in anion-exchange chromatography, Anal. Chim. Acta 398 (1999) 153–160.
[6] R. Tucceri, An electrochemical study of the nickel hydroxide-gold modified electrode employing the surface resistance technique, J. Electroanal. Chem. 774 (2016) 95–101.
[7] D. Tench, L.F. Warren, Electrodeposition of conducting transition metal oxide/hydroxide films from aqueous solutions, J. Electrochem. Soc. 130 (1983) 869–872.
[8] K.L. Chopra, Thin Film Phenomena, McGraw-Hill Co., New York, 1969.
[9] R. Tucceri, A review about the surface resistance technique in electrochemistry, Surf. Sci. Rep. 56 (2004) 85–157.
[10] J. Taraszewska, G. Roslonek, Electrocatalytic oxidation of methanol on a glassy carbon electrode modified by nickel hydroxide formed by ex-situ chemical precipitation, J. Electroanal. Chem. 364 (1994) 209–213.
[11] M. Fleishmann, K. Korinek, D. Pletcher, The oxidation of organic compounds at a nickel anode in alkaline solution, J. Electroanal. Chem. 31 (1971) 39–49.
[12] D.H. Angell, T. Dickinson, The kinectics of ferrous/ferric and ferri/ferrocyanide reactions at platinum and gold electrodes: part I, kinectics and bare-metal surfaces, J. Electroanal. Chem. 35 (1972) 55–72.
[13] C. Deslouis, B. Tribollet, in: H. Gerischer, C. Tobias (Eds.), Advances in Electrochemical Science and Engineering, Vol. 2, VCH Publishers, New York, USA 1992, p. 205.
[14] D.A. Szánto, S. Clerhorn, C. Ponce-de-León, F.C. Walsh, The limiting current for reduction of ferricyanide ion at nickel: the importance of experimental conditions, AIChE J 54 (2008) 802–810.
[15] J.O. Zerbino, C. de Pauli, D. Posadas, A.J. Arvía, Ellipsometry of nickel hydroxide electrodes formed by ex situ chemical precipitation. Potential routine and time effects, J. Electroanal. Chem. 330 (1992) 675–691.
[16] B. Paxton, J. Newman, Variable diffusivity in intercalation materials, a theoretical approach, J. Electrochem. Soc. 143 (1996) 1287–1292.

[17] J.W. Weidner, P. Timmerman, Effect of proton diffusion, electron conductivity, and charge-transfer resistance on nickek hydroxide discharge curves, J. Electrochem. Soc. 141 (1994) 346–351.
[18] S. Motupally, C.C. Streinz, J.W. Weidner, Proton diffusion in nickel hydroxide films. Measurement of the diffusion coefficient as a function of state of charge, J. Electrochem. Soc. 142 (1995) 1401.
[19] S. Motupally, Measurements of Diffusion Coefficient of Proton in Nickel Hydroxide Films as a Function of the State of Charge, University of South Carolina, USA, 1994 (Ph.D Thesis).
[20] S. Motupally, C.C. Streinz, J.W. Weidner, Proton diffusion in nickel hydroxide. Prediction of active material utilization, J. Electrochem. Soc. 145 (1998) 29.